Vein textures and chemistry of ore minerals associated with high grade gold mineralization from A east pit, Chatree gold deposit, Central Thailand

Phinyaphat Rongkhapimonpong*, Chakkaphan Sutthirat and Weerasak Lunwongsa

Department of geology, Faculty of Science, Chulalongkorn University, Bangkok, Thailand
Corresponding author e-mail: Phinyaphat.R@gmail.com

Abstract

Quartz texture, mineral assemblages and chemical compositions of ore minerals in A east pit of Chatree deposit were investigated to characterize the high grade gold mineralization. The deposit is characterized by quartz-carbonate-chlorite-adularia-pyrite veins and breccias intruding volcaniclastic sedimentary to andesitic volcanic breccia. Gold and electrum form as inclusion, fine-grained and mainly concentrated in pyrite host, based on quartz textural and petrological analysis. Adularia occur as multiple-phase inclusion of gold in pyrite host and rhodochrosite occur as gangue mineral and associated with gold bearing sulphide. The vein samples studies also associated with telluride enriched in electrum grain. Mineralized of quartz with a various textures includes banding, plumose, comb-zonal, moss, ghost-sphere and saccharoidal texture. The banded and plumose quartz texture are most closely associated with high grade gold and the most common texture of the vein samples studies.

Keywords: Quartz texture, High grade gold, Chemistry, Chatree gold deposit, Thailand

1. Introduction

Chatree gold mine is one of the largest epithermal gold-silver deposit in the central Thailand, which was green field discovery in 1995 and subsequently developed to operation in 2000. It is located on the eastern edge of the Tertiary Chao Phraya Basin (Diemar, 1999), 280 km north of Bangkok. Initial mineralization in Chatree deposit studies using core samples in D, C and H pits were made by Dedenczuk, 1998; Greener, 1999; Kromkhun, 2005. The detailed in vein texture and stage of vein in Q pit are studied by Tangwattananukul et al. (2009) and A pit are studied by Sangsiri (2010). There was subsequent detailed description of mineralogy and paragenesis covering the whole of the Chatree by Salam (2011), together with the other previous work of Salam (2006) and Cumming et al. (2008).

According to the intersected a broad zone of high grade gold mineralization in A pit, results include an intersection of 49.4 metres @ 4.3g/t gold (from 227 metres), including a high grade interval of 29.8 metres @ 6.25g/t gold (from 246 metres), from diamond drill hole of the year 2013. The high grade mineralization confirms the additional exploration drill holes in order to evaluate the potential of the deposit towards the east part of A pit (personal communication, 2013). Resource development drilling has identified targeting extensions and deeper gold mineralization in A east pit and required the vein characteristic related to high grade Au. The relatively high gold grade occurrences hosted in quartz veins were identified on the A east load ore body which is currently being mine as an open pit and located in Chatree north. Vein samples in these studies were examined in the difference between higher to lower gold grade. This studies are aimed at defining the vein characteristics in term of vein texture, sulphide and gangue mineral assemblages and chemical compositions to provide important information for targeting high grade gold mineralization.

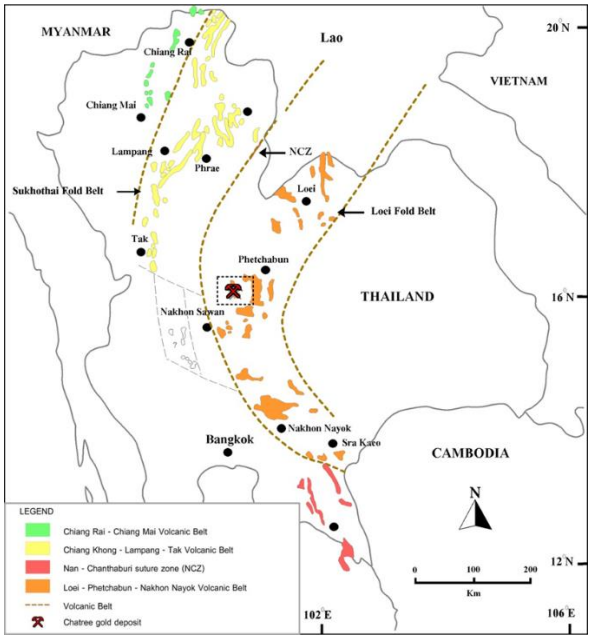

Fig. 1. Map of Thailand showing location of Chatree deposit in Loei Fold Belt (modified from Panjasawatwong et al., 1997).

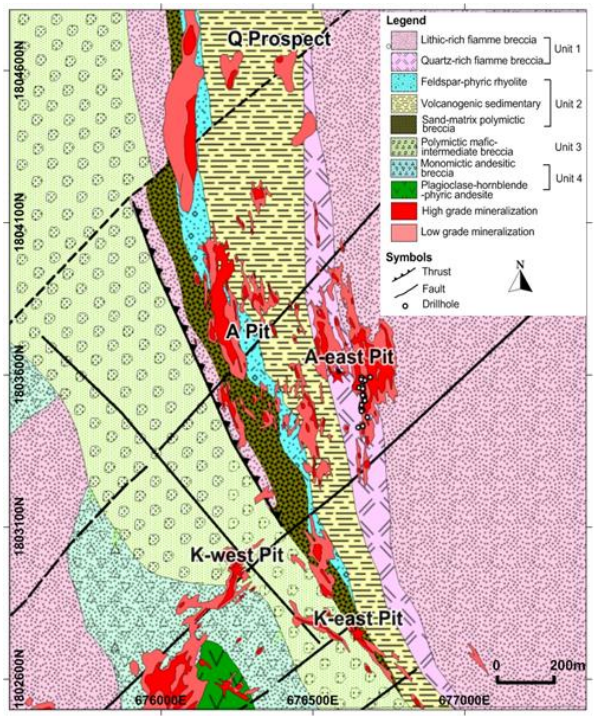

Fig. 2. Geological map of Chatree deposit showing the volcanic units and ore lenses (modified after Salam, 2011).

2. Geological setting

The Chatree epithermal Au-Ag deposit is located in the Loei-Petchabun volcanic belt (Fig. 1; Panjasawatwong et al., 1997) in the Late Paleozoic to Early Mesozoic and extend in north-south of central Thailand (Jungyasuk and Kositanont, 1992; Charusiri et al., 2002). The Loei-Phetchabun Volcanic belt is thought to have originated during the northward subduction of a large ocean basin (Paleo-Thethys) beneath the Indochina Terrane during the Late Permian and Triassic (Intasopa, 1992; Metcalfe, 1996). The Chatree Au mineralization have occurred in source and composition of magma is marked by a mixed volcano-plutonic magmatism at the Late Permian-Early Triassic (260-240 Ma, dated using Laser Ablation ICP-MS U-Pb zircon techniques by Salam et al., 2014).

The Chatree deposit contains seven major lithological components from the oldest to youngest (Cumming, 2004; Cumming et al., 2008; Salam et al., 2014): (i) Carboniferous volcanogenic sedimentary rocks and Lower Permian limestone; (ii) Late Permian plagioclase–hornblende-phyric basaltic andesite (unit 4); (iii) Late Permian polymictic mafic–intermediate breccia (unit 3); (iv) Upper Permian to Lower Triassic volcanogenic sedimentary unit (unit 2); (v) Late Permian to Early Triassic fiamme breccia (unit 1); (vi) Middle Triassic diorite and post-mineralization dykes and (vii) Upper Triassic and Jurassic Khorat Group.

The paragenetic sequence of mineralization identification based on cross-cutting relationship and characteristic of mineralize in the Chatree deposit, was presented by Salam (2011), who classified a seven-stage of vein: Stage 1: microcrystalline quartz + pyrite; Stage 2: (Stage 2A) quartz-chlorite-sericite-pyrite and (Stage 2B) quartz-sericite ± chlorite-chalcopyrite-pyrite-sphalerite ± galena; Stage 3: quartz - carbonate - (K-feldspar) ± carbonate ± sulphide; stage 4: (Stage 4A) quartz-chlorite ± carbonate ± adularia-sulphide-electrum, (Stage 4B) quartz ± carbonate-adularia-sulphide-electrum and (Stage 4C) carbonate ± quartz-

adularia – sulphide – electrum - argentite-tetrahedrite; Stage 5 quartz ± carbonate veins; Stage 6 quartz ± carbonate veins; and Stage 7 quartz-zeolite-carbonate.

The main gold-silver mineralization of Chatree is closely associated with Stage 4 (Salam, 2011) and characterized by colloform-crustiform banded quartz ± carbonate ± chlorite ± adularia-sulphide-electrum vein (Corbett et al., 2002; Salam, 2011; Salam et al., 2014).

The study area is A east pit which is in the eastern part of A pit area and located in the northern part of Chatree deposit (Fig. 2).The A east pit is underlain by Late Permian plagioclase–hornblende-phyric basaltic andesite (unit 4) and overlain by late Permian to early Triassic fiamme breccia (unit 1). The high Au grade in the large of ore zone favorable hosted in volcanogenic sandstone and laminated with pervasive silica, Salam (2011). The majority of mineralized veins trend N-S to NNW-SSE with dips of 60° to 85° to the west (gentle west dipping in the western part of the A Pit, steeper in A pit to A east pit), suggested data from field mapping by Salam (2011). The main gold mineralization of A pit include mainly colloform-crustiform banded and breccia of quartz ± carbonate ± chlorite-sulphide-electrum, massive vein and stockwork of quartz-carbonate±adularia-sulphide-lectrum, Sangsiri (2010).

3. Sampling and analytical techniques

Revisiting extremely high Au grade interval of the diamond drill core by the logging mineralization prior to samples selection. Forty of vein samples were collected from diamond drill cores that include vein, stockwork vein, breccia vein and banded vein in volcaniclastic sedimentary hosted taken in the A east ore zone. The vein selected sampling are re-analyzed for Au grade at Chatree laboratory. These study concentrated the gold grade greater than 8 g/t Au, present a grade of gold ranging from 1-73 g/t Au (relatively higher Au grade) and also selected small amount samples of the lowest gold grade between 0.1-0.9 g/t. The study of high grade vein in forty drill core sample has focused on mineral characteristic related to the main gold mineralization stage of Chatree gold deposit which follow the last updated vein paregenesis of Salam (2011).

All of forty vein samples were prepared as 46 thin section and 37 polished section for petrographic study. For sulphide chemistry study, 10 samples were collect for EPMA analysis. The petrographic and ore-petrography investigation aimed to identify the mineral relationship including vein texture, mineral assemblage, mineral composition, replacement and intergrowth, especially in quartz, sulfide and adularia under a polarizing microscope.

Ten polished section are selected for the electron-probe microanalysis or EPMA analysis (WDS: wavelength-dispersive spectroscopy) to enable analyses of sulphide minerals composition and sulphide phase related to gold mineralization. The ten polished section are prepared from ten representative of vein samples (8.8-73 g t^{-1} Au) which are the top of high Au grade samples and contain high concentration of sulphides. Mineral chemistry were analyzed using a JEOL JXA-8100, with accelerating voltage of 15kV and a probe current of 24 nA. There were used to produce an electron beam with a diameter of 1 µm (at the sample surface) to analyze the mineralized grains at department of geology, faculty of Science, Chulalongkorn University. This study is a quantitative analysis, result reported in element weight percent (Table 1, 2). The standards set used for electron microprobe were pure metals (Au, Cu and Ag), oxide (Al_2O_3 (Al), MgO (Mg), SiO_2 (Si), Cr_2O_3 (Cr), MnO_2 (Mn), $BaSo_4$ (Ba), $Ni2O_3$ (Ni), PbO (Pb), MoO_2 (Mo), mineral ($CaSiO_3$ (Ca), Fe_2SiO_4 (Fe), $NaAlSi_2O_6$ (Na), ZnO (Zn),

K_2O (K)) and internal standard (Te, Sb, Th, Ti, As, Se). This analysis also reported as oxides of elements (Table 3), such as plagioclase-feldspar, that use a procedure for calculating a chemical formula by Deer et al. (1978).

4. Results

4.1 Quartz texture

Quartz textures found associated with grade of gold mineralization in A east pit are defined on the basis of mutual geometrical relations among individual crystal, crystal form and the internal features of individual grains (Dong et al., 1995). The quartz texture observable in core-samples and under the micro-scope, can be divided into five major groups (Q1-5 group). The five major groups of quartz texture will be described from the relatively lower to higher gold grade as below (Fig. 3).

Q1: Saccharoidal/rhombic calcite

Saccharoidal texture display as milky fine-grained quartz matrix or crypto-crystalline quartz with subhedral to anhedral crystal in difference distribution by microscopic study. The saccharoidal texture is process from carbonate soluble with decreasing temperature in the early precipitation then replaced by silica-quartz mineral that are interpreted in the replacement texture, noted by Dong et al., 1995. Rhombic calcite occur as a late-stage filling or cross-cutting and show as breccia matrix. Both of saccharoidal and rhombic calcite show relative low gold grade between 0.1-3.7 g t^{-1} and consist of quartz ±grey silica, carbonate with small amounts of electrum and sulphide under microscope.

Q2: Moss/ghost sphere

Moss and ghost sphere show as sphere with ranging from 0.1-1.0 mm (in size) and characterized by aggregate of quartz crystal under microscope observation. Ghost sphere texture may referred as a special moss texture in the same characteristic of spherical distribution in amorphous silica or chalcedonic-quartz, noted by Dong et al., (1995). Ghost sphere texture under microscopic shows the radial extinction that may occur from silica gel crystallized to flamboyant texture. Moss/ghost sphere has a low Au concentration between 0.8-2.7 g t^{-1} and consist of quartz, chlorite, feldspar, dominantly pyrite and minor sulphide composition (±chalcopyrite, sphalerite, galena, tetrahedrite/tennantite and electrum)

Q3: Comb/zonal

Comb texture observed in few samples, show comb texture with prismatic and variable grained size of euhedral growth zone, and developed in a parallel orientation. The morphology of quartz crystal is a parallel orientation and perpendicular to vein walls (Dong et al., 1995). Zonal quartz texture can observed in the samples and show the individual euhedral quartz crystal, similar to comb textures with the prismatic growth zoning. The Q3 texture based on gold assay interval is consistent with moderate grade (5.9-6.6 g t^{-1}Au) and associated with quartz, carbonate, sericite, pyrite, chalcopyrite, sphalerite, galena and tennantite.

Q4: Plumose (feathery-flamboyant)

Plumose is the most abundant texture and has been defined as feathery, Adams (1920), Sander and Black (1988). The feathery texture is a recrystallization of amorphous silica to chalcedonic quartz and show variable of subhedral-euhedral quartz crystal in a prismatic grain forming (Dong et al., 1995). The feathery display as a patches throughout quartz crystal. The term of flamboyant is also similar to the feathery texture by Adams (1920), Sander and Black (1988). The flamboyant is characterized as radial or extinctions of quartz crystal with the rounded grain forming when observed under microscope. The plumose texture vein has a range of gold content from 3.0 up to 14.5 g t^{-1}, characterized by medium to coarse grained white, prismatic quartz (±chalcedonic) and parallel oriented in internal zoning,

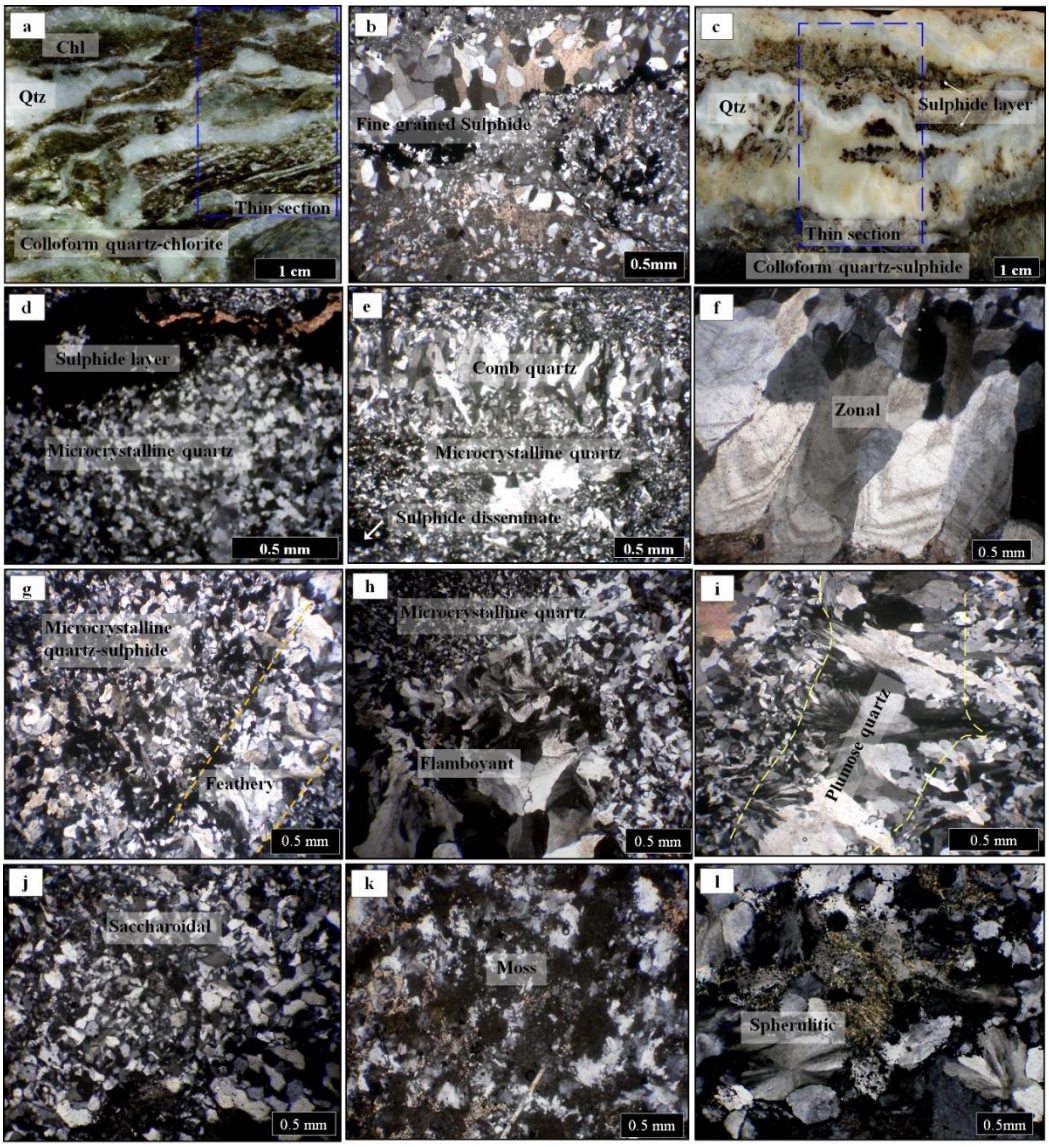

Fig. 3. Various textures of quartz in vein samples from A east pit, Chatree deposit, Thailand: a) A specimen showing colloform quartz (Qtz), green chlorite (Chl) banded vein and disseminated pyrite, and photomicrograph show as b) coarse grained quartz (upper) infilled by calcite, fine-grained sulphide disseminated and occur as layering along coarse-graind quartz band. c) A specimen showing colloform quartz-sulphide banded and photomicrograph show as d) sulphide layer in crystalline quartz. e) Microcrystalline quartz and disseminated sulphide cross-cut by coarse-grained comb quartz texture. f) zonal texture: individual euhedral, coarse grained quartz. g) Fine crystalline quartz-sulphide (center) intergrowth with coarse crystalline, feathery quartz texture (at right). h) Microcystalline quartz and disseminated sulphide intergrown with coarse crystalline, flamboyant texture. i) Microcrystalline quartz cross-cut by coarse grained, plumose quartz texture. j) Saccharoidal texture (randomly subhedral crystals distribution). k) Moss texture: spherical distribution of fine to coarse crystal quartz. l) Spherulitic texture of crystalline quartz associated with strong disseminated sulphide and sericitic alteration (yellow).

associated with adularia (feldspar), sericite, ±chlorite±carbonate and sulphide (pyrite, chalcopyrite, sphalerite, galena, tennantite and electrum).

Q5: Banding (crustiform-colloform)

Banding has characterized by crustiform and colloform texture and some layering has slightly brecciation. The term crustiform band comprising a narrow (up to a few centimeters) and sub-parallel band. Crustiform is a fine banding of microcrystalline quartz and comb quartz that developed from both wall. The colloform occur as concentric curve and under microscopic show fine-grained and coarse-grained quartz overgrowth texture. The banded texture can observed by the apparent of hand specimens. The crustiform and colloform are the second most common mineral texture and composed of quartz-grey quartz-co_3-sulfide, quartz-co_3-chlorite-sulfide banded vein with a dominantly of chlorite, feldspar, adularia and sulphide (mainly pyrite, chalcopyrite, sphalerite and tennantite). The banded vein texture has the most gold occurrence effect high grade gold, that have a relatively higher range of gold content between 3.8-73 g t^{-1}.

4.2 Mineral assemblage

Based on the stages of mineralization of Chatree deposit by Salam (2011), mineral composition especially in sulphide species of vein samples from A east pit, can be sub-divided the mineral assemblage into four major groups and represent sulfide and gangue mineral assemblages (Mineral assemblage group I, II, III and IV).

Assemblage group I, consists of quartz ±grey silica, carbonate and trace sulphide associated with small amount of electrum which occur in vein breccia and vein-veinlet in volcanic sedimentary breccia host and some massive carbonate vein in white colored with non sulphide concentration. This assemblage has a low gold grade (less than 1 g t^{-1}) that is the lowest rang of gold intercept in the vein selected samples.

Assemblage group II, occur similar to assemblage I with the minor sulphide composition (±chalcopyrite, sphalerite, galena and tetrahedrite/tennantite), but mineral assemblage II has the composition of chlorite, feldspar and dominantly pyrite and more Au content between 0.5-6.5 g t^{-1}. The chlorite occur as filling open-space, vein fragment supported in the quartz vein breccia. Both assemblage group I and II were obtained from vein stage 1 of Salam (2011). The vein stage 1 shows as clasts in the main gold stage (4A, 4B and 4C), Salam (2011).

Assemblage group III, is predominantly quartz-sericite and quart-(±sericite)-feldspar (adularia) with pyrite, chalcopyrite, sphalerite, galena ± tennantite and ±chlorite. The vein stage 2 and stage 3 of Salam (2011) are similar in composition to mineral assemblage III. The assemblage III has quite high Au grade in average of 3.7-9.8 g t^{-1} and occur most frequently in the plumose texture.

Assemblage group IV, has a dominantly in quartz, chlorite, feldspar, adularia and sulphide (pyrite, chalcopyrite, sphalerite, tennantite and electrum) which are the main sulphide and gangue minerals associated with main gold-silver mineralization stage (Stage 4A, 4B, 4C) of the Chatree deposit (Salam, 2011). The assemblage IV has relatively high gold content more than 3.8 g t^{-1} to the highest gold grade in 73 g t^{-1} Au (average of 16 g t^{-1} Au). The mineral assemblage IV is characterized by crustiform-colloform banded and subordinated with plumose texture.

4.3 Chemistry of ore minerals

Microscopic observation of sulphide minerals and spot chemical analysis by electron probe micro-analysis (EPMA) were performed on selected ore minerals from the banded and plumose quartz texture related to higher Au grade. EPMA point analysis can confirm mineral characteristic, chemical

Table 1. Chemical composition of the representative electrum (±telluride rich) in pyrite, based on electron probe microanalysis.

Mineral	(± Telluride rich) Electrum in Pyrite												
Sample point	A1_El1	A2_Au1	A2_Au2	A10_Au1	A10_Au2	A12_Au1	A12_Au3	A13_Au1	A24_El1	A24_El4	A38_El1	A38_El2	A38_El4
Analysis (Wt.%)													
Au	3.088	0.084	0.362	7.520	0.271	18.603	0.131	14.260	17.777	34.610	35.418	12.063	17.089
Ag	7.404	0.005	-	9.006	0.008	18.630	0.020	10.638	18.357	33.613	34.031	41.960	12.995
Fe	36.602	11.392	41.048	32.219	42.818	24.206	41.339	29.107	25.230	11.799	11.137	3.394	27.943
S	49.291	16.822	57.008	50.235	55.373	37.888	57.824	42.754	37.427	19.291	19.006	16.262	41.041
Mo	0.586	0.193	0.703	0.599	0.723	0.600	0.618	0.750	0.439	0.243	0.239	0.145	0.473
As	0.165	0.024	-	-	0.082	0.008	-	-	0.081	-	0.015	-	0.040
Zn	0.108	0.089	-	0.067	0.041	-	-	0.070	0.405	0.091	-	14.926	0.314
Cu	0.264	0.071	0.008	0.031	0.064	0.124	0.047	0.126	0.000	0.125	0.126	0.071	-
K	0.054	16.229	0.041	0.039	0.028	-	-	-	-	-	-	-	-
Al	0.047	10.303	0.022	0.064	-	-	-	-	0.042	0.059	0.053	0.094	0.031
Si	0.076	31.318	0.007	0.012	-	-	-	-	-	-	0.011	8.728	0.010
Mg	0.016	0.022	0.022	-	-	-	-	-	-	-	-	-	-
Te	0.042	-	0.007	0.219	-	-	-	0.151	0.228	0.181	0.003	0.035	0.095
Sb	0.090	0.697	-	-	-	-	-	-	-	-	-	-	-
Na	0.099	0.133	0.026	0.036	0.033	-	-	-	0.016	-	-	-	-
Mn	0.035	0.229	0.070	-	-	-	-	-	-	-	0.023	-	-
Ca	-	11.268	0.081	-	-	-	-	-	-	-	-	-	-
Se	0.026	-	-	-	-	-	-	-	0.003	0.048	-	-	-
Total	98.002	98.879	99.405	100.047	99.441	100.059	99.979	97.856	100.005	100.060	100.062	97.678	100.031
Atomic Prop.													
Au	0.016	0.000	0.002	0.038	0.001	0.094	0.001	0.072	0.090	0.176	0.180	0.061	0.087
Ag	0.069	0.000	-	0.083	0.000	0.173	0.000	0.099	0.170	0.312	0.315	0.389	0.120
Fe	0.655	0.204	0.735	0.577	0.767	0.433	0.740	0.521	0.452	0.211	0.199	0.061	0.500
S	1.537	0.525	1.778	1.567	1.727	1.182	1.803	1.333	1.167	0.602	0.593	0.507	1.280
Mo	0.006	0.002	0.007	0.006	0.008	0.006	0.006	0.008	0.005	0.003	0.002	0.002	0.005
As	0.002	0.000	-	-	0.001	0.000	-	-	0.001	-	0.000	-	0.001
Zn	0.002	0.001	-	0.001	0.001	-	-	0.001	0.006	0.001	-	0.228	0.005
Cu	0.004	0.001	0.000	0.000	0.001	0.002	0.001	0.002	0.000	0.002	0.002	0.001	-
K	0.001	0.415	0.001	0.001	0.001	-	-	-	-	-	-	-	-
Al	0.002	0.382	0.001	0.002	-	-	-	-	0.002	0.002	0.002	0.003	0.001
Si	0.003	1.115	0.000	0.000	-	-	-	-	-	-	0.000	0.311	0.000
Mg	0.001	0.001	0.001	-	-	-	-	-	-	-	-	-	-
Te	0.000	-	0.000	0.002	-	-	-	0.001	0.002	0.001	0.000	0.000	0.001
Sb	0.001	0.006	-	-	-	-	-	-	-	-	-	-	-
Na	0.004	0.006	0.001	0.002	0.001	-	-	-	0.001	-	-	-	-
Mn	0.001	0.004	0.001	-	-	-	-	-	-	-	0.000	-	-
Ca	-	0.281	0.002	-	-	-	-	-	-	-	-	-	-
Se	0.000	-	-	-	-	-	-	-	0.000	0.001	-	-	-
Total	2.304	2.944	2.530	2.280	2.507	1.890	2.552	2.038	1.895	1.310	1.295	1.564	2.000

- Concentration below detection limit.

component of the visible and invisible accumulation of Au, Ag and sulfide species. Most common type of gold in high grade gold mineralized samples from A east pit occur as electrum (Au, Ag) in pyrite, Table 1, Fig. 4a. Pyrite is the main host of electrum inclusion to fine-grained dissemination, whereas sphalerite is subordinate hosts of gold and electrum as the fine-grained and small inclusion. Pyrite commonly found as individual, porous masses (spongy network) and crystalline pyrite (in size from 50-1000um), which associated with quartz-chlorite-sericite (altered feldspar), electrum and other sulphides. The pyrite form as fine grained inclusion of gold content in the K-feldspar host (Fig.4b). Pyrite dominates and comprises about 40-50 wt. % of total sulphide with the molybdenite (Mo) and aresenic(As) up to 0.68% , 0.17% respectively. The electrum grains (Fig. 4c) are formed as fine to very fine grained, and irregular shape, ranging from 2-20 microns with 0.13-35.42 wt. % of Au and less than 0.001-34.031 wt. % of Ag. The maximum content of Au and Ag

occur in irregular shape of electrum in Mo rich pyrite with a ratio to 1.75 of Ag/Au.

Sphalerite founded at the second most inferior to pyrite. The sphalerite displays irregular, reniform shape and filamentous texture (0.05 to 0.2 mm). Sphalerite is typically associated with pyrite, chalcopyrite galena and tennantite. The sphalerite forms as pure sphalerite (ZnS) in dark grey colored in a common with Fe content ranging from 1.47-2.53 wt%(3-4 mol% FeS) and nil to 0.07 wt% Au. The Fe-rich sphalerite(ZnFeS) is observed in quartz-adularia-sericite-black sulphide vein to vein breccia in a feathery quartz to banded vein and have Fe content

Table 2. Chemical composition of the representative sphalerite and tennantite, based on electron probe microanalysis.

Mineral	Sphalerite							Tennantite	
Sample point	A11_Sp1	A11_Sp2	A17_Sp1	A32_Sp1	A38_Sp1	A38_Sp2	A38_Sp3	A010_Sf1	A024_Sf1
Analysis (Wt.%)									
Au	0.066	-	-	0.440	-	-	-	0.422	0.130
Ag	-	-	-	1.235	-	-	-	0.024	0.024
As	-	0.038	-	0.056	0.043	-	0.008	1.291	0.020
Mo	0.500	0.520	0.525	0.641	0.478	0.519	0.514	0.707	0.724
Zn	54.840	55.642	56.245	20.003	55.084	53.253	53.993	0.092	0.072
Cu	0.778	0.117	0.681	0.066	0.286	0.840	0.781	0.092	0.069
Te	-	0.148	0.101	-	-	0.072	-	-	-
Fe	1.943	1.670	2.530	26.064	1.524	1.466	1.658	41.922	41.422
S	37.961	37.869	36.227	50.085	38.392	38.661	38.502	55.019	56.282
Na	2.422	2.434	2.380	0.830	2.471	2.467	2.466	0.075	0.019
Al	-	-	0.077	0.439	-	-	0.006	-	0.002
Tl	0.351	0.245	0.213	-	0.049	-	0.307	0.177	-
Mn	0.099	0.143	0.093	-	0.079	0.086	0.065	-	-
K	-	-	-	-	0.067	0.045	0.058	0.135	-
Se	-	-	-	-	-	-	-	0.007	-
Total	98.960	98.826	99.072	99.859	98.406	97.364	98.300	99.963	98.764
Atomic Prop.									
Au	0.000	-	-	0.002	-	-	-	0.002	0.001
Ag	-	-	-	0.011	-	-	-	0.000	0.000
As	-	0.001	-	0.001	0.001	-	0.000	0.017	0.000
Mo	0.005	0.005	0.005	0.007	0.005	0.005	0.005	0.007	0.008
Zn	0.839	0.851	0.860	0.306	0.842	0.814	0.826	0.001	0.001
Cu	0.012	0.002	0.011	0.001	0.005	0.013	0.012	0.001	0.001
Te	-	0.001	0.001	-	-	0.001	-	-	-
Fe	0.035	0.030	0.045	0.467	0.027	0.026	0.030	0.751	0.742
S	1.184	1.181	1.130	1.562	1.197	1.206	1.201	1.716	1.755
Na	0.105	0.106	0.104	0.036	0.107	0.107	0.107	0.003	0.001
Al	-	-	0.003	0.016	-	-	0.000	-	0.000
Tl	0.002	0.001	0.001	-	0.000	-	0.002	0.001	-
Mn	0.002	0.003	0.002	-	0.001	0.002	0.001	-	-
K	-	-	-	-	0.002	0.001	0.001	0.003	-
Se	-	-	-	-	-	-	-	0.000	-
Total	2.184	2.180	2.161	2.409	2.188	2.176	2.186	2.504	2.509

- Concentration below detection limit.

reaches to 26.06 wt% (46 mol% Fes), Au up to 0.44 wt% and Ag up to 1.24 wt%, Fig.4d, Table 2.

Chalcopyrite ($CuFeS_2$) founded as subhedral to anhedral in a brassy yellow to yellow colour and associated with pyrite, galena, sphalerite and tennantite. The chalcopyrite also replace and corroded pyrite, and intergrowth with sphalerite and galena. The multistage inclusion of chalcopyrite coexist with galena and tennantite. The chalcopyrite contain up to 0.43 wt% Au and 0.30 wt% Ag (Fig.4e).

Galena is in the light grey colour as observed in microscopic study. It has a white and lighter grey colored against tennantite in

pyrite and sphalerite crystals. The galena also occur as a small inclusion(less than 0.01mm) in tennantite (Fig.4d). The galena have not the presence of gold concentration.

Tennantite distributed as small rounded inclusion in a characteristic feature of light to medium grey colour with a bluish tint, and red internal reflection in pyrite. The tennantite shows as single and multiphase inclusion (0.01-0.02mm) with chalcopyrite and electrum in pyrite crystal (Fig.4f) and has abundant in quartz-sericite and quartz-chlorite. The proportions of gold is also present as invisible gold in tennantite (Fig.4f, sample A10_sf1 as Table 2). This sample shows the correlation between set of element consist copper (Cu), arsenic (As) and sulfur (S) that represents the chemical composition

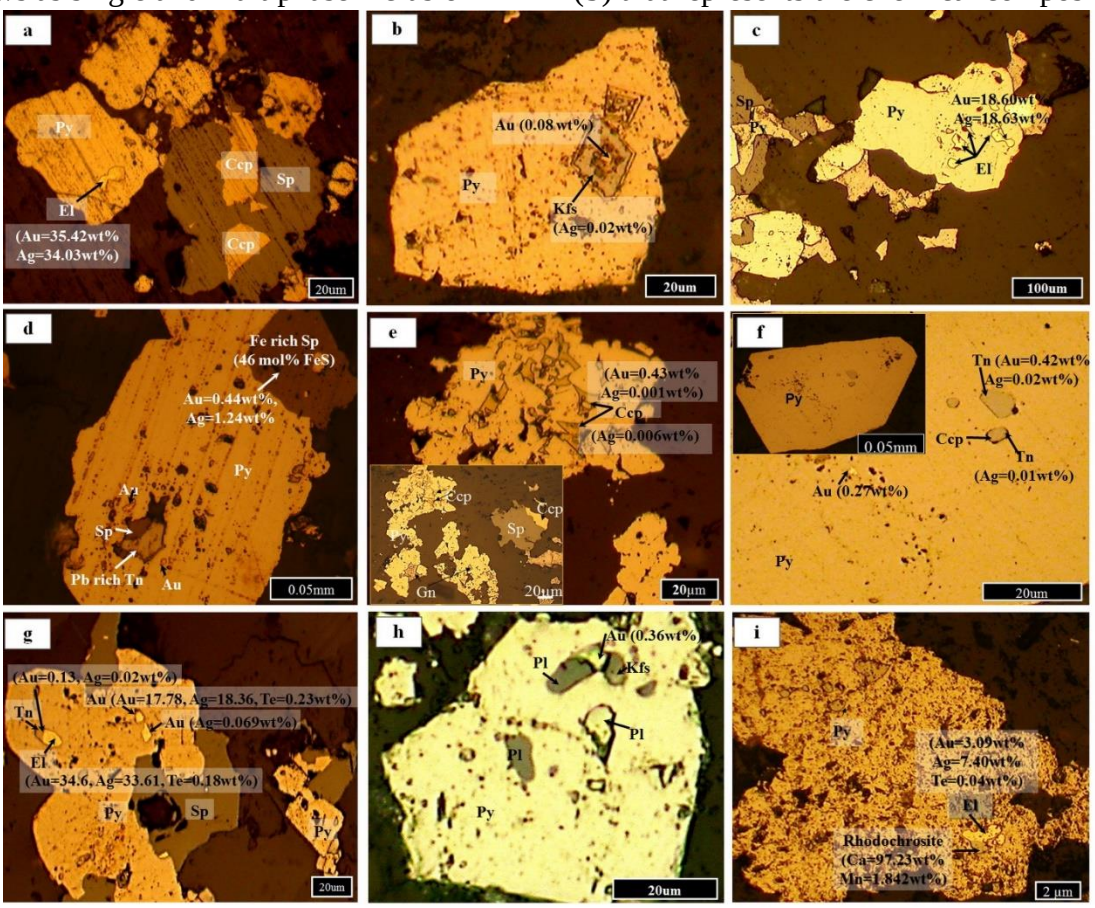

Fig. 4. Photomicrograph of high grade vein mineralization from the A east pit, Chatree deposit a) Electrum (El) inclusion in Mo rich pyrite, (A38_El1). b) Multiple phase inclusion of gold-pyrite (Py) in rhombic K-feldspar crystal (adularia habit); A2_Au1 and A2_Sf1. c) Fine-grained gold and gold inclusion in Mo rich pyrite; Table 1 (A12_Au1- A12_Au3). d) Fe-rich sphalerite (Sp) hosted fine-grained gold concentration (A32_Sp1). e) Fine-grained gold-telluride (Te) in chalcopyrite (Ccp). f) Multiple phase inclusion of gold-tennantite (A10_sf1, A10_sf2). g) Telluride-electrum attached to tennantite (Tn) inclusion (left). Gold inclusion in pyrite crystal at right. (A24_El1 and A24_El2 for Au (centre), A24_El4 for El-Te(left) attached to tennantite (A24_sf1). h) Gold inclusion in pyrite enclosed to K-feldspar (Kfs) and plagioclase (Pl); A2_Au2 (gold inclusion), A02_fsp1 (plagioclase), A02_fsp2 (K-feldspar); Table3. The plagioclase feldspar form as inclusion in pyrite. (A02_fsp3 at left and A02_fsp4 at right). i) Inclusion of gold (A1_El1) and Ca, Mn rich carbonate (rhodochrosite) in grey colored (A01_Sf1) in (spongy) pyrite host.

of tennantite ((CuFe).As.S. In addition, electrum occur with tennantite as multi-stage inclusion in pyrite crystal (Fig.4g) in the colloform quartz-chlorite vein.

Potassium feldspar and plagioclase feldspar composition develop as inclusion and enclosed to gold inclusion in pyrite crystal in quartz carbonate-sulphide banded vein and vein breccias with silicification.

The K-feldspar in rhombic shape founds with multiple phase inclusion of gold and pyrite (Fig.4b, sample A2_Sf1 as Table 3). K-feldspar and plagioclase feldspar inclusions enclosed to gold. The plagioclase feldspar also form as inclusion in pyrite host from the result of A02_fsp3 and A02_fsp4; Fig.4h. EPMA analyses of feldspar and recalculated formula based on 8 oxygens are given in Table 3.

Rhodochrosite (Mn-carbonate) occur as inclusion with a grain size of 1 micron in light to medium grain colored and intergrown with

Table 3. Chemical composition of K-feldspar and plagioclase feldspar, based on electron probe microanalysis.

Mineral	K-feldspar			Plagioclase feldspar		
Sample point	A02_Py2	A02_Sf1	A02_fsp2	A02_fsp1	A02_fsp3	A02_fsp4
Analysis (Wt.%)						
SiO_2	67.75	67.25	68.24	21.04	54.15	37.75
Al_2O_3	8.69	16.74	17.40	6.01	14.71	12.94
FeO	1.69	0.13	0.17	0.47	0.22	1.08
MnO	0.00	0.04	0.11	2.68	0.38	1.81
MgO	0.77	0.00	0.17	0.78	0.05	2.30
CaO	0.84	0.12	5.11	63.65	20.72	38.47
Na_2O	0.16	0.15	0.07	0.06	0.07	0.04
K_2O	13.19	13.26	6.95	4.28	7.94	4.46
Total	93.08	97.69	98.21	98.97	98.23	98.85
Formula 8(O)						
Si	3.33	3.11	3.07	1.32	2.67	2.04
Al	0.50	0.91	0.92	0.44	0.86	0.82
Fe^{2+}	0.07	0.00	0.01	0.02	0.01	0.05
Mn	0.00	0.00	0.00	0.14	0.02	0.08
Mg	0.06	0.00	0.01	0.07	0.00	0.18
Ca	0.04	0.01	0.25	4.28	1.10	2.22
Na	0.02	0.01	0.01	0.01	0.01	0.00
K	0.83	0.78	0.40	0.34	0.50	0.31
Total	4.84	4.83	4.67	6.63	5.15	5.71
Atomic %						
An	4.97	0.76	37.84	92.45	68.40	87.74
Ab	1.71	1.68	0.88	0.15	0.41	0.16
Or	93.32	97.56	61.27	7.40	31.19	12.10

electrum (Au=3.09 and Ag=7.40 wt.%, Fig.4i) in pyrite host under the micro-scope. The result from EPMA data of calcium-rich rhodochrosite has a concentration of 97.23 wt. % Ca, 1.84 wt. % Mn and 0.13 wt% Au. The rhodochrosite associated with quartz-sulphide band and carbonate replacement and has not visible rhodochrosite in the hand specimen (25 g t^{-1}Au).

Telluride occur as a small inclusion in electrum in Mo rich pyrite host, Table 1. Exemplification as EPMA sample no. A024_El4 comprises maximum Au reach to 34.61 wt. % of Au, 33.61 wt. % of Ag (Au-Ag ratio of 1:1.77) and 0.18 wt. % of tellutide (Te) that related to telluride rich electrum enclosed with tennantite inclusion in pyrite (Fig.4g). The telluride rich electrum occur in banded vein to vein breccias of quartz-chalcedony-carbonate-±adularia sulphide (pyrite-chalcopyrite-sphalerite).

The telluride rich electrum has all six EPMA point samples, based on EPMA analysis (Table 1), can be give a general formula as $(Au_{0.31}Ag_{0.69})Te_{0.014}$, $(Au_{0.60}Ag_{1.82})_{1.43}Te_{0.01}$, $(Au_{0.36}Ag_{0.63})_1Te_{0.03}$, $(Au_{0.50}Ag_{0.95})_{1.46}Te_{0.01}$, $(Au_{0.22}Ag_{1.42})_{1.64}Te_{0.01}$, $(Au_{0.47}Ag_{0.65})_{1.11}Te_{0.004}$ of EPMA sample A10_Au1, A13_Au1, A24_El4, A24_El1, A38_El2 and A38_El4 respectively, with Ag/Au ratio of 1.36-2.19

5. Discussion and conclusion

Mineralization texture and gold deposit

The goal of this study was to examine mineralize characteristic in term of mineralize texture and mineralize composition that related to high grade gold mineralization. Five types of quartz texture of gold mineralization in A east are defined in this study. Based on a detailed petrography study of quartz texture and sulphide occurrence in quartz vein from A east pit of Chatree deposit, the colloform banded quartz texture which relatively higher Au (4.1-73.0 g t^{-1}Au) and most associated with the sulphide assemblage IV (chlorite-adularia-feldspar-pyrite-sphalerite-chalcopyrite-tennantite-electrum). Similarly, the main gold-silver mineralization stage of the Chatree deposit (studied by Salam, 2011);

Stage 4A: quartz - chlorite ± carbonate ± adularia –sulphide - electrum, Stage 4B: quartz ± carbonate-adularia-sulphide-electrum and Stage 4C carbonate ± quartz-adularia-sulphide-electrum-argentite-tetrahedrite. Sulphide and electrum tend to be enriched in the quartz-chlorite rich band with subordinate enrichment in the quartz± carbonate band. The sulphide-rich chlorite-quartz band tends to have a high Au grade by petrographic observation (Salam, 2011).

The most common plumose quartz texture has range of gold grade (3.0-14.5 g t^{-1} Au) and mainly has association of sulphide mineralize assemblage III and IV. The plumose occur more frequently in high grade Au (average of 8.8 g t^{-1}). Both plumose and banded are the most common of quartz texture observed in 25 of 40 samples in high grade vein of A east. Previous studies (Kilias et al., 2013) have suggested the colloform band and plumose texture are most closely associated with high concentration of Au. Similarly to the epithermal Ag-Au deposits at Guanajuato, Mexico that studied by Moncada et al., 2012 who reported the plumose and banded is closely to higher Au and Ag grades. The study of Vearncombe (1993) revealed that the crustiform-colloform banding and plumose or acicular crystal are the characteristic of open-space filling for gold deposition.

The previous study discuss the process of generating the colloform texture relate to gold bearing. The high grade Au in this study occur in fine-grained quartz-sulphide bands and is deposited by rapid cooling and possibly fluid mixing which has been reported by Ovenden et al., 2005. The mixing of hydrothermal fluid with bicarbonate is a resulting gold precipitated, that Leach and Corbett (2008) introduced the term of bonanza Au in epithermal vein deposited by mixing of ore fluid with low pH water. Corbett (2002) reported the bonanza Au often occur in epithermal quartz-sulphide bands with electrum-rich bands.

The sulphide assemblage III (sericite-pyrite-sphalerite-chalcopyrite-tennantite ±electrum) also shows association texture with comb and zonal texture related to high gold grade (range of 5.9-6.6 g t^{-1} of Au). In contrast, the comb and zonal textures are identified in to the phase of non- boiling textures as slow crystal growth that related to the lower Au grade, (Moncada et al., 2012). The Pajingo epithermal vein systems studied by Pinder (2006), show a concentration of Au grade is commonly below 1.0 g t^{-1} in comb texture. Due to a low population of comb and zonal texture containing, that they have not a clear correlation between high or low Au grade. This is compatible with the studied of quartz texture at Q and A pit in Chatree deposit by Tangwattananukul (2012), which show that the comb and flamboyant (plumose) texture associated with large amount of sulphide and electrum whereas the colloform banded from A pit described by Sangsiri (2010) most associated with the high gold grade.

The moss and ghost-sphere have lower Au grade in range of 0.8-2.7 g t^{-1} and is recognized in sulphide assemblage II (minor sulphide; pyrite, sphalerite), and developed by spherulitic crystallization into the wall rock. The Moss (ghost-sphere) texture displays in the early stage vein texture and may form precipitated during or immediately after banded quartz vein texture occurrence (Ovenden et al., 2005). It can indicate that the moss texture have not enough time and condition to produce higher concentration of gold deposit.

Relatively low Au (0.1-3.7 g t^{-1}) of saccharoidal quartz texture are associated with mineralize assemblage I (microcrystalline quartz- trace amount of pyrite). The microcrystalline quartz is classified as vein Stage 1 of Salam (2011), who interpreted the effect of rapid cooling on microcrystalline quartz precipitation. The mineral assemblage I can be regarded as a precursor stage of the main gold mineralization stages, Salam (2011). Similarity, Bunikasih low sulphidation epithermal system studied by Subandrio et al. (2010) that the saccharoidal texture has relatively low range of gold (0.3-3.1 g t^{-1}). Braund, 2006 interpreted the low grade gold and are indicative of more quiescent condition.

The Au grade is lower in the saccharoidal (assemblage I) and moss/ghost-sphere (assemblage II) of quartz vein textures that show small amounts to trace of sulphide (pyrite-sphalerite-galena) and have effected a grade of gold. As mentioned by Salam (2011), that the presence of sulphides is probably an indication of a high gold content.

Mineral chemistry association of high grade gold mineralization

The assemblage IV observed in A east, such as quartz**,** chlorite, adularia, feldspar, pyrite, sphalerite, chalcopyrite, tennantite and electrum in the plumose and colloform banded texture, indicate the main phase of gold deposition and most associated with the high Au grade. Also, electron-microprobe analyses of mineral assemblage IV can be confirmed mineral characteristic, chemical component of the visible and invisible accumulation of Au, Ag and sulfide species that associated with gold mineralization.

Associated mineral chemistry by EPMA analyses revealed that the high grade gold (electrum) mineralization at Chatree deposit in A east pit are recognized into 6 mineralize assemblages: (1) Electrum in Mo rich pyrite (±As), (2) Electrum-K-feldspar (adularia) in Mo rich pyrite, (3) Electrum-(Fe-rich) sphalerite, (4) Electrum-sulfosalt(tennantite), (5) Telluride rich-gold-electrum and (6) Gold-rhodochrosite.

Electrum occurs predominantly as inclusions in molybdenum (Mo) rich pyrite with subordinate amounts of arsenic (As). Salam (2011) studied pyrite chemistry in Chatree deposit and suggested the molybdenum (Mo) occurs in the pre-mineralization stages, whereas arsenic (As) occur in both pre-mineralization and main gold mineralization stages. In this study, the Fe-poor sphalerite has much a lower Au content (0-0.07 wt.% of Au, 3-4 mole% FeS) than the Fe-rich sphalerite (0.44 wt.% of Au, 46 mole% FeS). It might be able fine grained gold bleb in late stage of Fe rich sphalerite formed, resulted from low temperature and higher salinity ore fluids in sulfur reducing conditions, as mentioned by Noku et al, 2012). Under such low temperature (~ 200 °C) conditions, the ore fluids have to be acidic (pH < 4) that probably increased the gold solubility ($Au(HS)_2^-$) as observed by Moss and Scott (2001).

The presence of adularia in Chatree deposit was reported previously by Sangsiri (2010) that show crystalline quartz bands associated adularia and disseminated sulphides and sulphide bands in A pit. Dong and Morrison (1995) reported the adularia is a low temperature polymorphism of K-feldspar and is an indicator of boiling in the epithermal system. Besides, the adularia also precipitates in the most of gold bearing quartz vein in A pit and Q prospect in Chatree deposit (Tangwattananukul, 2012).

The tennantite associated with gold-electrum, same as mentioned by Salam (2011) from Chatree gold deposit and Braund (2006) from Cracow deposit in Queensland. The tennantite has a very low Sb (0.007 wt. %) that can be detected as the

phase composition very close to tennantite ($Cu_{12}As_4S_{13}$), suggested by Moritz, 2006. It is characterized by high As content reaches to 1.29 wt. % and also high Fe content that still called tennantite.

The telluride in this study common found as inclusion of tennantite (hessite (Ag_2Te). Bogdanov et al. (2005) studied in Au-Ag-Te-Se minerals at Bulgaria and described the hessite is closely associated with gold. Correspondingly, the Craccow, epithermal gold deposit, also has the hessite association with electrum and occur in the quartz banded vein, as mentioned by Braund (2006) who studied the Ag-Te phase of low sulphidation. From studied of chemical composition and zoning of pyrites by Salam (2011), suggested that Te probably form as Au-Te inclusions in pyrite.

6. Acknowledgement

The authors thank Issara Mining Ltd., for financial, technical support, and permission to work in research, especially Genesio Circosta, Fiona Davidson, Brendan Badley. The autors thank Saranya Nuanla-ong for teaching me in selected sampling and vein paragenesis, Phuriwit Sangsiri for teaching me in microscopes and understanding of quartz texture, Alongkot Funka and Sopit Pumpuang for their assistance in EPMA analysis and logistical support, staffs of Issara Mining for their help with collecting samples. Thanks to Jensarin Vivatpinyo for her support, encouragement and suggestion in discussion manuscript. The authors also thank Dr. Abhisit Salam at Department of Geology, Chulalongkorn University for review comments and suggestion in petrography and geochemical manuscript.

7. References

Adam, S.F., 1920. A microscopic study of vein quartz. Economic Geology, 15.

Braund, K.G., 2006. Geology, Geochemistry and paragenesis of the Royal, Crown and Roses Pride low sulphidation epithermal quartz vein structures, Cracow, South-East Queensland. Unpublished Thesis, University of Queensland, 1-334 pp.

Charusiri, P., Daorerk, V., Archibald, D., Hisada, K. and Ampaiwan, T., 2002. Geotectonic evolution of Thailand, a new Tectonic feature of Eastern Thailand synthesis. *Geological Society of Thailand*, 1: 1-20.

Corbett, G., 2002. EPITHERMAL GOLD FOR EXPLORATIONISTS. *AIG Journal*, Applied Geoscientific Practice and Research in Australia, 1: 1-26.

Cumming, G.V., 2004. Analysis of volcanic facies at the Chatree gold mine and in the Loei- Phetchabun Volcanic Belt, central Thailand. Unpublished Honours Thesis, University of Tasmania, 84 pp.

Cumming, G.V., James, R., Salam, A., Zaw, K., Meffre, S., Lunwongsa, W., Nuanla-Ong, S., 2008. Geology and mineralisation of the Chatree epithermal Au-Ag deposit, Phetchabun and Phichit Provinces, central Thailand, *Proceeding of PACRIM Congress 2008*, Australian Institute of Mining and Metallurgy, Gold Coast, Australia, pp. 409-416.

Dedenczuk, D., 1998. Epithermal gold mineralisation at Khao Sai, Phichit, Thailand. Unpublished Honours Thesis, University of Tasmania, Australia

Deer, W.A., Howie, R. A., Zussman, J., 1978. An Introduction to the Rock-Forming Minerals, England, 528 pp.

Diemar, M.G. and Diemar, V.G., 1999. Geoloogy of the Chartee Epithermal Gold deposit, Thailand, *Pacific Rim Conference 1999*, Indonesia, pp. 227-231.

Dong, G., Morrison, G., Jaireth, S., 1995. Quartz Texture in epithermal veins, Queensland: classification, origin, and implication, 90, 1841-1856 pp.

Greener, S., 1999. Wall-rock alteration and vein mineralogy of C-Zone, a low-sulphidation Au-Ag epithermal deposit in the Chatree Prospect, Thailand. Unpublished Honours Thesis, Tasmania.

Intasopa, S., 1993. Petrology and geochronology of the volcanic rocks of central Thailand volcanic belt. Unpublished PhD Thesis, University of New Brunswick, Canada, 242 pp.

Jungyusuk, N., Khositanont, S., 1992. Volcanic rocks and associated mineralisation in Thailand, *Proceedings of National Conference on Geologic Resources of Thailand*: Potential for Future Development, pp. 522-538.

Kilias, S.P., Paktsevanoglou, M., Giampouras, M., Stavropoulou, A., Apeiranthiti, D., Mitsis, I., 2013. Gold occurrence, mineral textures and ore fluid properties at the Viper (Sappes) epithermal Au–Ag–Cu ore body, Thrace, Greece, 12th SGA Biennial Meeting 2013. *The Society for Geology Applied to Mineral Deposits (SGA)*, At Uppsala, Sweden.

Kromkhun, K., 2005. Geological setting, mineralogy, alteration, and nature of ore fluid of the H-zone, the Chatree deposit, Thailand. Unpublished M.sc Thesis, University of Tasmania, Australia.

Metcalfe, I., 1996. Gondwanaland dispersion, Asian accretion and evolution of eastern Tethys. *Journal of Asian Earth Sciences*, 43: 605-623.

Moncada, D., Mutchler, S., Nieto, A., Reynolds, T. J., Rimstidt, J. D., Bodnar, R. J., 2012. Mineral textures and fluid inclusion petrography of the epithermal Ag–Au deposits at Guanajuato, Mexico: Application to exploration. *Journal of Geochemical Exploration*, 114(0): 20-35.

Moritz, R., 2006. Fluid salinities obtained by infrared microthermometry of opaque minerals: implications for ore deposit modeling. *Journal of Geochemical Exploration* 89: 284–287.

Moss, R., Scott, S. D., 2001. Geochemistry and mineralogy of gold-rich hydrothermal precipitates from the eastern Manus Basin, Papua New Guinea. Can. Mineral, 39: 957–978.

Noku, S.K., Matsueda, H., Akasaka, M. and Espi, J. O., 2012. Petrology, Geochemistry, and Fluid Inclusion Microthermometry of Sphalerite from the Laloki and Federal Flag Strata-Bound Massive Sulfide Deposits, Papua New Guinea: Implications for Gold Mineralization. Resource Geology 62(2): 187–207.

Ovenden, A., Baker, T., Mustard, R., Bolt, S., 2005. Textural and geochemical analysis of veins in the Pajingo epithermal system, Queensland, Australia in Discrimination of barren versus gold-bearing epithermal systems and vectoring of ore in the Pajingo mining area, 63, EGRU (Economic Geology Research Unit) Contribution, 63, James Cook University.

Panjasawatwong, Y., Chantaramee, S., Limtrakun, P., Pirarai, K., 1997. Geochemical and tectonic setting of eruption of central Loei volcanics in the Pak Chom area, Loei, northeast Thailand: Proceeding of International conference on Stratigraphy and tectonic evolution of Southeast Asian and the South Pacific, Bangkok, *Proceeding of International conference on Stratigraphy and tectonic evolution of Southeast Asian and the South Pacific, Bangkok*, pp. 287-302.

Pinder, J., 2006. Geochemical evaluation and modelling of the macro to micro-scale variations of the Vera Nancy system, Pajingo, North Queensland Australia. Unpublished Honours Thesis, James Cook University of North Queensland, 148 pp.

Salam, A., 2006. A Geological, Geochemical and Metallogenic study of the Northern Chatree area, Phetchabun province, Loei fold Belt, Central Thailand – progress report, In: Geochronology, Metallogenesis and Deposit Styles of Loei Fold belt in Thailand and Laos PDR, CODES: ARC

Linkage Project, CODES Centre for Excellence in Ore deposit Research, University of Tasmania.

Salam, A., 2011. A Geological, Geochemical and Metallogenic study of the Chatree epithermal deposit, Phetchabun province, Central Thailand. Unpublished Thesis, University of Tasmania (UTAS), Australia, 1-251 pp.

Salam, A., Zaw, K., Meffre, S., Mcphile, J., Lai, C.K., 2014. Geochemistry and geochronology of the Chatree epithermal gold–silver deposit: Implications for the tectonic setting of the Loei Fold Belt, central Thailand. *Gondwana Research*, 26(1): 198-217.

Sander, M.V., Black, J.E., 1988. Crystallization and recrystallization of growth zoned vein quartz crystals from Epithermal systems-implication for fluid inclusion studies. *Economic Geology*, 83.

Sangsiri, P., 2010. Wall rock Alteration and Mineralization of the A and the H West Prospects, Chatree Gold Deposit, Phichit and Phetchabun, Province, Central Thailand. Unpublished M.sc Thesis, Chulalongkorn University.

Subandrio, A.S., Basuki, N.I., 2010. Alteration and Vein Textures Associated with Gold Mineralization at the Bunikasih Area, Pangalengan, West Java. Indonesian *Journal on Geoscience*, 5(4): 247-261.

Tangwattananukul, L., 2012. Characteristic features of gold mineralization at the Chatree deposit, Central Thailand. Unpublished Thesis, Akita University, Japan 1-103 pp.

Vearncombe, J.R., 1993. Quartz vein morphology and implications for formation depth and classification of Archaean gold-vein deposits. *Ore Geology Reviews*, 8(5): 407-424.